

IN-PROCESS PORTABLE PHOTOGRAMMETRY USING OPTICAL TARGETS FOR LARGE SCALE INDUSTRIAL METROLOGY

¹Ibai Leizea-Alonso, ²Jon Zubizarreta-Gorostidi, ¹Alberto Mendikute-Garate, ³José-Antonio Yague-Fabra

¹IK4-Ideko. (Spain)

²CEIT-IK4 (Spain)

³IA, University of Zaragoza (Spain)

DOI: <http://dx.doi.org/10.6036/9401>

1.- INTRODUCTION

Portable photogrammetry is increasingly used as a 3D measurement technique in industrial metrology applications for large manufacturing components [1,2]. In previous work [3,4] a photogrammetry-based process was presented with the aim of reducing manual intervention in machine alignment of raw parts before machining. The process starts out of machine with the measurement of the raw part. Photogrammetry takes images around the part to which a set of optical markers placed on its surface have been added. The traceability of the system is given by cameras and scale bars (each containing a pair of optical markers with known distance, thus achieving the actual scale of the scene) previously calibrated by a post-processing. According to the detection of the 2D coordinates of the optical markers, it is possible to determine the position and relative orientation of the camera for each of the images, along with the calculation of the 3D coordinates of each of the optical markers. The best-fit is also obtained of the raw part with respect to the ideal design of the part (see Figure 1) [4].



Figure 1. Portable photogrammetry for out-of-machine measurement of raw components before large machining [4].

Camera calibration is a relevant factor contributing to measurement uncertainty [1,5,6]. Accurate calibration of the camera model (also referred to as intrinsic or internal parameters) is required. In addition, the measurement depends on the thermo-mechanical stability of the structure on which the cameras are available, as well as the corresponding process of calibration of extrinsic parameters for each camera (relative position of each camera).

On the one hand, when using pre-calibrated cameras with optical markers, there are two main limitations: economical cost and long computing times, due to the need for photogrammetric adjustment (*bundle adjustment*) [7,8]. The latter is a limitation and makes it difficult to implement in an efficient industrial measurement process. However, when using low-cost commercial cameras without optical markers and approximate self-calibration, accuracy is limited.

In this article, a solution is proposed that integrates low-cost cameras and optical markers. The objectives of the work are: first, to improve computational efficiency including an in-process self-calibration method, that is, to run in real time without post-processing. The solved 3D point cloud is used as calibration geometry, avoiding the need for specialized pre-calibrated cameras outside the process. Second, obtain a self-calibration procedure using redundant information available in the measurement provided by the optical markers to obtain the required accuracy.

2.- MATERIALS AND METHODS

Portable photogrammetry calculates the 3D coordinates of a set of optical markers placed on an object [9.10] based on its 2D coordinates in image. Multiple photos of an object are taken from different camera points of view. By detecting the 2D coordinates of optical markers in different images, it is possible to calculate the camera positions and orientations for each of the photos (called extrinsic parameters) and calculate the 3D coordinates of the markers by triangulation from multiple points of view. The traceability of the measurement is established by a defined set of scale bars, with calibrated lengths between pairs of optical markers arranged on them, together with precise calibration of the camera model (called intrinsic parameters) [11-15].

In this work (see Figure 2), two low-cost digital cameras are used, a Nikon D300S (4288 x 2848 pixels, 12MP 5.5'm 24 mm) and a Xiaomi A1 mobile (4000 x 3000, 12MP 1.25'm 4 mm).

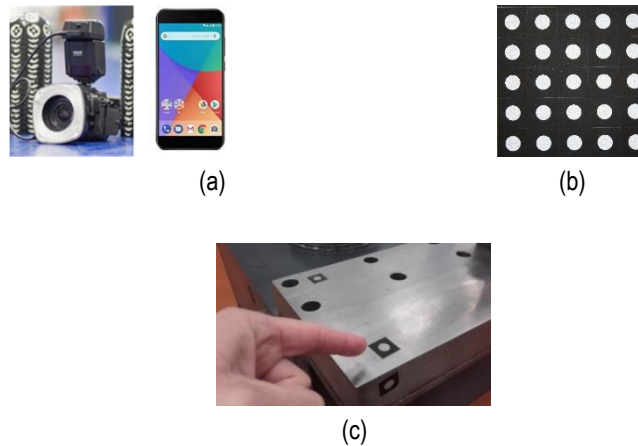


Figure 2. Measuring instrument in portable photogrammetry. (a) Digital cameras (Nikon 300S and Xiaomi mobile), (b) adhesive optical markers, and (c) optical markers on the reference part.

Figure 3 shows the reference part used in this job to evaluate the accuracy of the self-calibrated portable photogrammetry process. This is a part (see Figure 3(a)) with four prismatic subitems of steel bolted to a mechanically welded structure and milled to nominal geometry (Figure 3(b)), the measurement volume of which reaches 1m³.

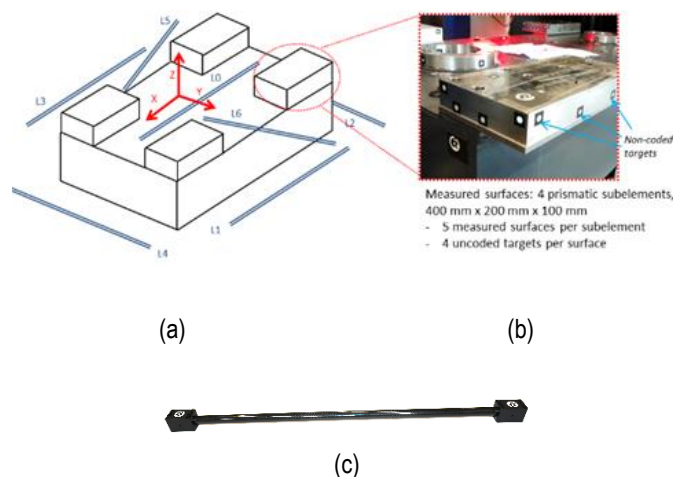


Figure 3. Reference part (a) analysed (1.5 m x 1 m x 0.5 m) with four prismatic subitems (400 mm x 200 mm x 100 mm) milled with an accuracy of 0.01 mm, along with a scale bar for the evaluation of LME (L0 to L6, average bar length of 930 mm), optical markers in the prismatic subitems (b) and example of a carbon fibre (c) scale bar.

In order to evaluate the measurement in a laboratory scenario (Figure 3a), an approximation of distance measurement errors (LME-*Length Measuring Error*) according to VDI 2634 [15], verifying the behaviour of the resolved markers (i.e. the 3D coordinates of optical markers). Six scale bars (L1 to L6) were placed around the scene (1.5 m x 1 m x 0.5 m) in two groups of three (L1 to L3 and L4 to L6), along with a scale bar in the centre of the scene (L0) as the only traceability element for approximate self-calibration. In addition, prismatic subitems (Figure 3b) were measured by placing optical markers on each of the milled surfaces. Subsequently, the 3D coordinates of the resolved optical markers were adjusted to each nominal geometry [3], and the errors for each nominal reference surface were evaluated.

Finally, the photogrammetric self-calibration system was verified in two industrial scenarios measuring raw parts up to 15 m long. The verification was carried out with reference to a stapling process integrated into the wear (with a repeatability of 10m) executed on relatively precise milling machines (assuming an uncertainty of 0.01 mm). Once the part was properly aligned, the machine coordinates of the optical markers were measured using the probe. Therefore, the errors between the machined values and the corresponding 3D coordinates resolved after measurement and adjustment were contrasted.

3.- RESULTS

This section describes the assessment of the computational strategy for the portable photogrammetry measurement process, with the incorporation into this strategy of the ability to self-calibration of intrinsic camera parameters based on redundant information available in images taken during the measurement process [4]. Both computational efficiency and measurement uncertainty achieved with the use of low-cost consumption cameras described in the previous section are evaluated.

3.1.- COMPUTATIONAL EFFICIENCY FOR IN-PROCESS RESOLUTION

The behaviour of photogrammetric adjustment (*bundle adjustment*) plays a relevant role in the development of an efficient computational process for portable photogrammetry. As presented in previous work [4], it is possible to adopt an efficient computing strategy each time a new photo is taken during the measurement process:

1. Image processing for detection of 2D coordinates in optical marker image and distortion correction.
2. Calculation of an initial approximation of the extrinsic parameters of a new image.
3. Given the extrinsic parameters of a new camera, calculating an initial approximation of the 3D coordinates of a new encoded optical marker.
4. Intermediate photogrammetric adjustment for the extrinsic parameters of the camera and the 3D coordinates resolved according to the images taken so far, using the approximations in steps 2 and 3. The measurement process continues with the acquisition of images, following steps 1 to 4 each time a new image is taken.
5. Assign code to each new bookmark between the images obtained so far.

Finally, once the measurement process is complete, a photogrammetric adjustment set of extrinsic parameters and 3D coordinates is calculated in post-process, along with the intrinsic parameters of the camera model. As a result, the traceability of the process is given by the distances of the calibrated scale bars that have been resolved in the scene. To model lens and camera distortion, highlight the wide adoption of the Brown model [16]. The distortion model, along with the focal length, form the so-called intrinsic camera parameters, which characterize camera conditions as a measuring instrument in photogrammetry. That is, brown model coefficients are calibrated, assuming first and second order radial distortion coefficients (K1 and K2), first-order tangential (P1 and P2), and main point image coordinates (cl, rw), offering characteristic values obtained for each camera and parameter model. The resolution method is proposed as a problem of minimizing back-project errors in images obtained by multivariate optimization in the direction of least squares using the Gauss-Newton method [10] of the 3D coordinates of optical markers, the extrinsic parameters of each image, and the intrinsic parameters. Each numerical iteration can be expressed according to the following equation

$$J^T J \Delta_{\theta} = -J^T r$$

where Δ_{θ} corresponds to the vector of independent variables to be optimized in the problem of minimization of residues in the sense of least squares, which in this case correspond to the extrinsic camera parameters of each image and the 3D coordinates of the optical markers, r corresponds to the vector of reprojection errors observed in all images for all markers to be resolved, and J is the Jacobian matrix characteristic of portable photogrammetry measurement geometry, composed of partial derivatives of each reprojection error equation of each marker observed in each image with respect to the 3D coordinates of the marker and the extrinsic camera parameters of the image.

The process described above was developed in C++ language, using the OpenCV library for image processing and the Eigen library for array processing, on an Intel Core i7-7600U 2.8 Ghz two-core computer (4 virtual cores in total), with 16 Gb RAM and running on Windows 10 64-bit. Wireless image transmission from each camera was also used, with a transmission time of approximately 0.5 to 1 s per image for images of approximately 12 megapixels.

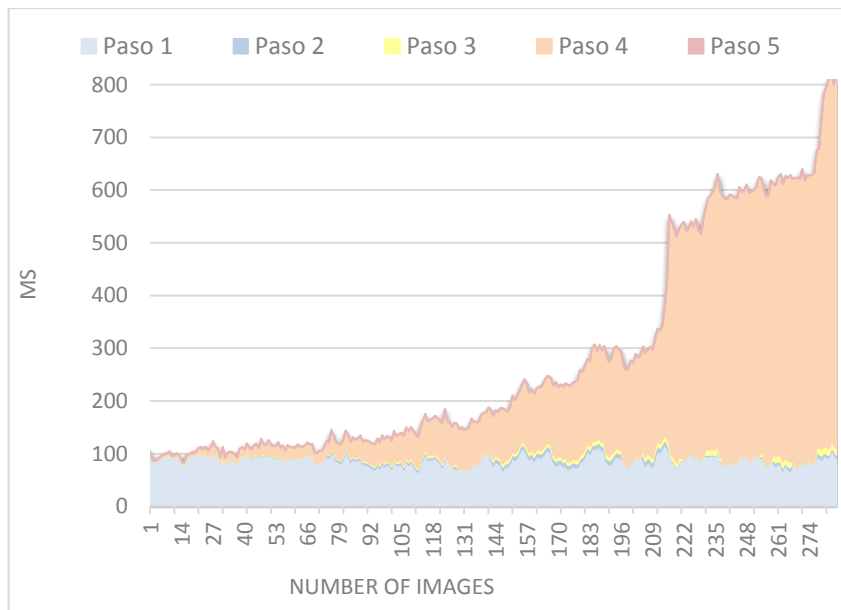


Figure 4 Cumulative area plot of the computational cost (in ms) of each step of the measurement system. The steps accumulate in order, resulting in the total computational cost.

Figure 4 shows the contribution of each step of the measurement system with an increasing number of images processed using current optimized algorithms. The first step is relatively constant (although it depends slightly on the number of optical markers observed in the image). In addition, steps 2, 3 and 5 hardly contribute to computational cost. However, you can see that the intermediate photogrammetric adjustment (step 4) it grows as the number of images resolved increases, becoming the task at the highest computational cost.

Compared to the approximation posed in [4], the algorithms used during all steps have been optimized by reducing unnecessary or avoidable calculations and parallelizing them in the most appropriate cases. For example, image processing (step 1) has been observed to reach 120 ms with many markers (up to 120 markers in a single image), below the previously presented 500 ms. However, these steps require about 90 ms on average. However, the higher computational cost focuses on intermediate photogrammetric adjustment (step 4), depending on the number of images accumulated and the coordinates of the markers. In any case, the total computing time is less than 1 second per image in the evaluated measurement scenario (Figure 3), allowing the measurement process to run efficiently, achieving a total post-processing measurement time below 5 minutes.

3.2.- SELF-CALIBRATION OF CAMERA IN PROCESS

Instead of using digital cameras specific to portable photogrammetry and requiring pre-calibration [9,10,12], the solution evaluated below enables in-process self-calibration [4] using redundant information available at the measurement scene.

This information is acquired by joint resolution of the 3D coordinates of the optical markers and the extrinsic parameters of each image.

Figure 5 shows the evaluation scenario according to the methodology presented in section 2 (Figure 3a). Both chambers were evaluated by the LME methodology.

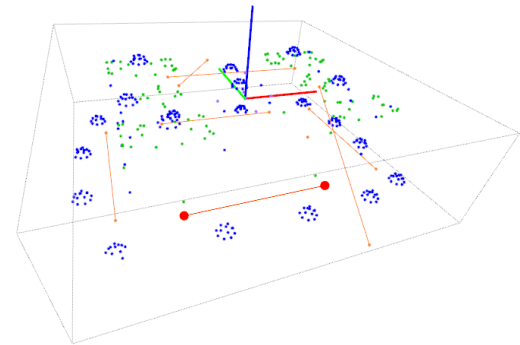
A maximum length measurement error of 0.89 mm ($\mu = 0.67$ mm and $\sigma = 0.17$) is observed in the photogrammetric measurement provided by the Xiaomi mobile camera, corresponding to a relative accuracy approximately 1/1,000 given by the 930 mm scale bars. Measurements were performed with an exposure time of 1/250 seconds (ISO 400), using the phone's built-in lighting.

For the Nikon D300S digital camera, better measurement performance was expected, due to the quality of the optics used (Nikkor lens) and the use of an active lighting ring allowing for lower exposure times and stable images, which contributes to better image quality during the manual measurement process. As a result, a maximum of 121.4 m of LME is observed, with a standard deviation of the entire set of scale bars of 45.1 m, leading to a relative precision of 1/10,000. According to the observed maximum value of 121.4 m, spatial uncertainty of the 3D coordinates of markers could be estimated at 70.1 m (σ), according to the law of propagation of variances for nonlinear functions without covariance can be shown to be $\sigma \cdot \text{LME} / \sqrt{3}$ and assuming a distribution of isotropic uncertainty on all three axes [17].

In any case, a relative accuracy of 1/10,000 per LME analysis is confirmed in the worst case for all spatial directions using a Nikon D300S on the standard part stage. This demonstrates that the accuracy of self-calibrating photogrammetry in process is appropriate, with the same performance for specialized pre-calibrated digital cameras mentioned in [9].



(a)



(b)

Figure 5 LME approximation for evaluation of the accuracy of the standard part. (a) Measuring instruments on the part. Scale bars arranged around the scene and in all spatial directions. (b) Representation of a measurement result, with the optical markers arranged in the part (in green) together with the evaluation of the scale bars (orange) and a scale bar for the traceability of the measurement process (red).

3.3.- EVALUATION IN INDUSTRIAL SCENARIOS

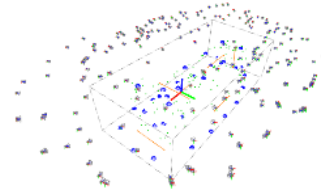
Finally, the complete process of part alignment based on self-calibrated photogrammetry in process was evaluated in an industrial scenario with two different parts (Figure 6). The goal was to demonstrate that the raw parts measurement process is fast, reliable and accurate. The system was applied to two raw parts before machining up to 15 m in length, at least an order of magnitude greater than the standard part (see Figure 3). The goal is to validate dimensional control of ± 1 mm overmaterial tolerances in working volumes up to 200 m³. Similarly, the Nikon D300S digital camera was used due to its previously observed high performance.

A total of approximately 800 markers and 200 images were resolved in both scenarios (see Figure 6). The performance of the in-process computing procedure was observed, with a maximum in-process computing time of almost 2s per image for the latest images during measurement processes, greater than 1s per image observed on the standard part stage. Even so, the proposed solution allows real-time diagnostics and control of images in an industrial scenario. The greatest contribution in increasing the time of the measure in process is the increase in the cost of intermediate adjustment in the latter stages of the measurement process. This result was expected due to the dependence on computational cost on the number of images and markers to be resolved.

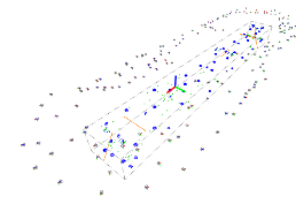
Regarding accuracy, according to the LME evaluation results presented in the literature [9], typical scale-dependent LME errors could be estimated at 50 m + 20 m/m for portable photogrammetry with pre-calibrated camera. In the industrial cases being considered, with parts up to 15 m long, a performance of approximately 0.35 mm could be expected as a reference for precise procedures, which would correspond to a spatial uncertainty of 0.20 mm (σ) for markers, assuming again that $\sigma \times \text{LME} / \sqrt{3}$.

Measurement performance was assessed in the same way as presented in Section 2. After measuring the raw part through photogrammetry, the part was precisely aligned with the coordinates of the corresponding machine. The photogrammetry measurement process was validated against a palpation measurement of a minimum set of 10 points, distributed in the 3 directions of the machine and on the extreme and opposite surfaces of the part. You could expect a 0.6 mm \pm error interval (3σ) according to the spatial uncertainty estimated by LME ($\sigma=0.20$ mm). The evaluation of the process was carried out by comparing the overmaterial resolved in the markers after the photogrammetric measurement process and fit with the machine-measured overmaterials using the

probe integrated into the head. In both industrial scenarios, all probing errors ranged below ± 0.5 mm, demonstrating the accuracy of the self-calibrated photogrammetry process for measuring and aligning large raw parts and controlling excess material.



(a)



(b)

Figure 6 Evaluation tests in an industrial scenario for two end users (Goimek and Liebherr). Large raw parts are displayed prior to machining. (a) Mobile column of the Soraluze milling machine (6 m long) manufactured in the Goimek machining workshop, and (b) Liebherr drilling rig lead centre (15 m long), together with the corresponding measurement results that together represent the 3D coordinates of the markers and the positions of the chambers.

4.- CONCLUSIONS

This work introduces additional steps towards an efficient procedure to solve the problem of photogrammetric adjustment (*bundle adjustment*) in portable photogrammetry. The processing capability of in-process photogrammetric adjustment has been demonstrated on a consumer laptop, enabling quasi real time 2D image and 3D scene computing and diagnosis. This ensures a reliable measurement process, allowing an easy, economical and fast solution for industrial metrology of large components.

Likewise, a technique of self-calibration of intrinsic parameters of in-process camera has been integrated, reaching precisions typical of pre-calibrated metric cameras with the use of consumer cameras (Nikon D300S and Xiaomi camera). Highlights the traceability of the measurement process where it is only set by the scale bars arranged in the scene. The photogrammetry process has been evaluated in two scenarios for measuring and aligning raw parts before machining: a standard part (1.5 m long reference part) and in two large-scale industrial scenarios (up to 15 m). A relative accuracy of 1/1,000 has been completed when using the Xiaomi mobile phone and 1/10,000 with the Nikon D300S (Nikkor optics). The latter with the same performance accuracy presented for portable photogrammetry with pre-calibrated cameras.

References

- [1] Schmitt R H, Peterek M, Morse E, Knapp W, Galetto M, Häting F, Goch G, Hughes B, Forbes A, Estler W T .Advances in Large-Scale Metrology—Review and future trends. CIRP Ann Manuf Technol. 2016.65, 643–665. Decentering distortion of lenses Decentering distortion of lenses Decentering distortion of lenses Decentering distortion of lenses [2] Uriarte L, Zatarain M, Axinte D, Yagüe-Fabra J A, Ihlenfeldt S, Eguia J, Olarra A. Machine tools for large parts. CIRP Ann Manuf Technol. 2013 62, 731–750. DOI: <https://doi.org/10.1016/j.cirp.2013.05.009>
- [3] Zatarain M, Mendikute A, Inziarte I. Raw part characterization and automated alignment by means of a photogrammetric approach. CIRP Ann Manuf Technol. 2012. 61, 383–386. DOI: <https://doi.org/10.1016/j.cirp.2012.03.137>
- [4] Mendikute A, Yagüe-Fabra J A, Zatarain M, Bertelsen A, Leizea I. Self-Calibrated In-Process Photogrammetry for Large Raw Part Measurement and Alignment before Machining. Sensors. 2017. 17, 2066. DOI: <https://doi.org/10.3390/s17092066>

- [5] Remodino F, El-Hakim S. Image Based 3D Modelling: A review. *Photogramm Rec.* 2016. 21, 269–291. DOI: <https://doi.org/10.1111/j.1477-9730.2006.00383.x>
- [6] Long C, Zhu J, Yi W. Portable visual metrology without traditional self-calibration measurement model. *Measurement.* 2016. 90, 424–437. DOI: <https://doi.org/10.1016/j.measurement.2016.05.017>
- [7] C. Engels, H. Stewénus, D. Nistér. Bundle adjustment rules. *Photogramm. Comput. Vis.*, 2006: pp. 266–271. DOI: <https://doi.org/10.1.1.126.6901>.
- [8] B. Triggs, P.F.P. McLauchlan, R.I. Hartley, A.W.A. Fitzgibbon. Bundle Adjustment—A Modern Synthesis. *Int. Workshop Vis. Algorithms*, 2000: pp. 298–372. DOI: <https://doi.org/10.1.1.37.6846>.
- [9] Luhmann, T. Close range photogrammetry for industrial applications. *ISPRS J. Photogramm. Remote Sens.* 2010, 65, 558–569. DOI: <https://doi.org/10.1016/j.isprsjprs.2010.06.003>
- [10] Hartley, R.; Zisserman. *A. Multiple View Geometry in Computer Vision.* Cambridge University Press: Cambridge, UK, 2003. DOI: <https://doi.org/10.1017/CBO9780511811685>
- [11] Babapour, H.; Mokhtarzade, M.; Zoj, M.J.V. Self-calibration of digital aerial camera using combined orthogonal models. *ISPRS J. Photogramm. Remote Sens.* 2016, 117, 29–39. DOI: <https://doi.org/10.1016/j.isprsjprs.2016.03.015>
- [12] Luhmann, T.; Fraser, C.; Maas, H.G. Sensor modelling and camera calibration for close-range photogrammetry. *ISPRS J. Photogramm. Remote Sens.* 2016, 115, 37–46. DOI: <https://doi.org/10.1016/j.isprsjprs.2015.10.006>
- [13] Huang, S.; Zhang, Z.; Ke, T.; Tang, M.; Xu, X. Scanning Photogrammetry for Measuring Large Targets in Close Range. *Remote Sens.* 2015, 7, 10042–10077. DOI: <https://doi.org/10.3390/rs70810042>
- [14] Herráez, J.; Denia, J.L.; Navarro, P.; Rodríguez, J.; Martín, MT. Determining image distortion and PBS (point of best symmetry) in digital images using straight line matrices. *Measurement* 2016, 91, 641–650. DOI: <https://doi.org/10.1016/j.measurement.2016.05.051>
- [15] VDI. VDI/VDE 2634: Optical 3D Measuring Systems—Part 1; VDI/VDE Guide Line. 2000. Beuth: Berlin, Germany.
- [16] Brown, D.C. Decentering distortion of lenses. *Photogramm. Eng. Remote Sens.* 1966, 32, 444–462.
- [17] Bureau International des Poids et Mesures (France). JCGM 100:2008. Evaluation of measurement data – Guide to the expression of uncertainty in measurement. BIPM, Sèvres (2008).

ACKNOWLEDGMENTS

We would like to thank Imanol Herrera (IK4-Ideko) for their contribution in the computational efficiency section for in-process resolution, as well as Iker Aguinaga (CEIT-IK4) for the revision of the article.